

Performance of Port Facilities in Southern Chile during the February 27, Maule Earthquake



S. Brunet, J.C de la Llera

Pontificia Universidad Católica de Chile, Chile

SUMMARY

This article describes the seismic performance of a group of ports in southern Chile during the February 27, 2010, Maule (Chile) earthquake. Research and field work was conducted for about a year after the earthquake and included a total of 14 ports located 95 km southwest of the epicenter. As it was observed in previous earthquakes, damage in piers and wharves were soil related and included soil liquefaction and lateral spreading. A number of structural failures also occurred, some of them attributed to soil factors and others to structural design aspects, such as short pile effects and natural torsion. This situation is contrasted herein with the performance of the South Coronel Pier, which was seismically isolated in 2007. The isolated portion of this port remained operative after the earthquake. Piles and superstructure remained within elastic range, while the isolators experienced important inelastic deformations.

Keywords: Chile Earthquake, Ports, Earthquake Damage, Seismic Isolation, Field Observation

1. INTRODUCTION

In the early morning of February 27, 2010 Chile was hit by an earthquake of magnitude $M_w = 8.8$, by now, the sixth largest in known seismic history (USGS, 2010). Inversion techniques using teleseismic data showed that the rupture was for the first time bilateral since previous Chilean earthquakes were known to rupture from north to south. The rupture included two main slip zones, one at latitude 36.187° S and longitude 72.676° W near the town of Cobquecura, and the other in the ocean at latitude 34.719° S and longitude 72.676° W near the city of Pichilemu; in both zones, the maximum slip was estimated at about 15 m (USGS, 2010).

Located 95 km south from the epicenter, Talcahuano and Concepción underwent a particularly strong ground shaking. This relative small geographic region concentrates 10% of the industrial ports in Chile (MOP, 2005). Damage to port facilities was particularly significant and was attributed to soil liquefaction, lateral spreading, pile structural failures, and pounding. Previous studies have demonstrated that the seismic behavior of port structures shows significant variability since the parameters that control the seismic behavior of soils are uncertain, and the seismic response and performance assessment of port structures is particularly challenging.

Among these port structures, the South Coronel Pier (SCP) is particularly interesting as a benchmark since it was seismically isolated. Built in 2007 with an isolation concept that combines vertical piles in parallel with elastomeric isolators placed on top of groups of four interconnected battered piles, SCP remained operative after the earthquake. The elastomeric isolators worked extremely well during the event, preventing important motions in the super-structure, as opposed to the poor performance of other port structures presented herein.

2. REVIEW OF EXISTING PORTS AND OBSERVED DAMAGE

The $M_w=8.8$ thrust fault earthquake occurred in the so-called Constitucion Seismic Gap (Ruegg et al., 2009) at the converging boundary between the Nazca (Pacific) and South American tectonic plates, with the former moving landward below the latter at converging rates of approximately 80 mm per year (U.S.G.S., 2010).

Two interesting accelerograms were registered in the cities of Concepción and San Pedro, 103 and 111 km southeast from the epicenter, respectively (Barrientos, 2010). The recorded peak ground accelerations (PGA) in the N-S, E-W, and U-D directions were 0.40g, 0.28g and 0.40g for Concepción; and 0.65g, 0.61g, and 0.58g for San Pedro, respectively. Shown in Figure 2.1 is a comparison between the resulting 5% damped response spectrum for these records and the design spectrum specified at the time by the National Seismic Code NCh433 Of.96 (INN, 1996). It is apparent that the earthquake response spectrum exceeds the NCh433 code for two period ranges: from 0 to 0.5s for both records and from 1.25 to 3s for horizontal components of the Concepción record. The earthquake is characterized also by large vertical components, which were larger than the horizontal components in many time instants, such as the short period range (0 to 0.5s).

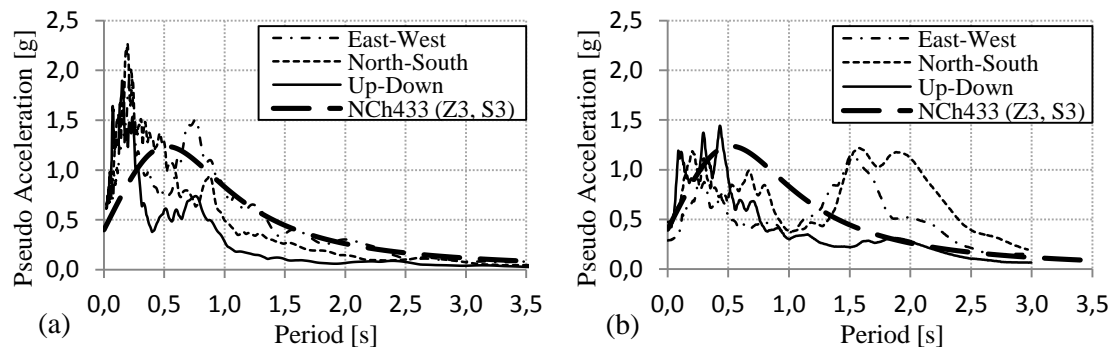


Figure 2.1. Comparison of NCh 433 design spectra and earthquake response spectra for records at: (a) San Pedro, and (b) Concepcion.

Summarized in Table 2.1 are some of the most relevant general properties of the different ports considered. Most of the ports are classified as open type structures, i.e., pile supported pier/wharfs, concrete decks and steel frames with conveyor belts or oil pipes, depending on their purpose, while the rest are quay walls and one small jetty.

Table 2.1. Principal characteristics of analysed ports

Port	Location	Cargo Type	Structure Type	Length(m)	Width(m)	N° Piles	Year
1	-36.70°, -72.98°	Container	Pile-supp. Pier	616	~ 10	451	1953, 1985*
2	-36.71°, -72.99°	Container	Pile-supp. Pier	710	~ 50	404	1995, 2000*
3	-36.76°, -73.00°	Bulk	Pile-supp. Pier	1783	3	157	1970
4	-36.71°, -73.10°	Container	Quay Wall	400	100	-	1935, 1973*
5	-36.69°, -73.09°	Navy	Quay Wall	740	360	-	1896
6	-36.73°, -73.13°	Container	Pile-supp. Wharf	20	605	782	1974, 1992*
7	-36.73°, -73.13°	Oil	Pile-supp. Pier	930	~ 6	~ 282	2009
8	-36.74°, -73.13°	Bulk	Pile-supp. Pier	374	27	1496	1949, 1974*
9	-37.03°, -73.17°	Bulk	Pile-supp. Pier	860	3	128	1991
10	-37.02°, -73.16°	Bulk	Pile-supp. Pier	770	4,5	~ 192	1942, 1985*
11	-37.05°, -73.17°	Bulk	Pile-supp. Pier	1115	3	128	2009
12	-37.02°, -73.15°	Fish Cove	Jetty	100	4	49	2000
13	-37.03°, -73.15°	Container	Pile-supp. Pier	541	30	317	1996, 2000*
14	-37.03°, -73.15°	Container	Pile-supp. Pier	645	37	312	2007

* Extension/upgrade

The most frequently observed damage in the ports can be classified as: (i) soil related, and (ii)

structural. Soil related problems such as liquefaction and lateral spreading were present in several structures. Among the most common structural problems included damage in pile-deck connections, especially in the bracing systems due to fracture of the welding or the reinforcement in pile heads and pile caps, stiffener buckling, loss of concrete cover, and pounding.

Soil liquefaction was perhaps the most frequently observed problem in these port structures. Settlement and inclination of sections of piers occurred repeatedly along the coastline due to the temporary loss of stiffness and bearing capacity of soils. As an example, Figure 2.2 presents the differential settlement of 17 pairs of piles placed on the approach zone of the East Lirquén Pier, causing a deformation of 40cm between axes A and C (at a distance of 138m and 228m from the abutment). The approach zone of the pier remained in good operative condition and diagonal cracking observed did not compromise the lateral stability for operational loads, but had to be repaired in order to restore the seismic lateral capacity of the pier.

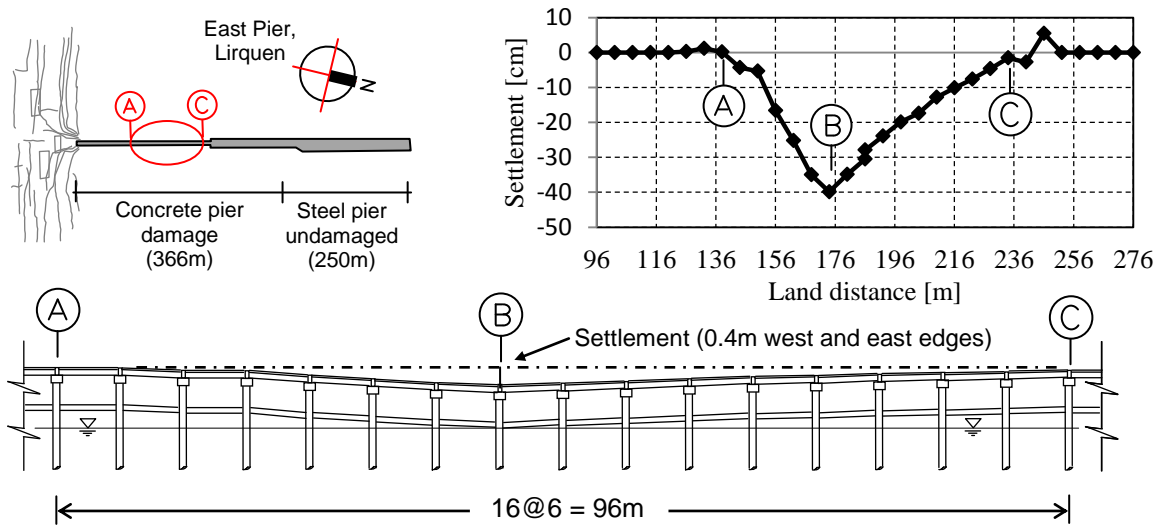


Figure 2.2. Settlement of the approach zone in Lirquén east pier due to liquefaction.

For ground shaking of this magnitude, soil liquefaction in saturated loose sands is almost inevitable. Furthermore, if soil layers happen to be on a certain slope, they will tend to slide down causing lateral spreading of the foundation system. Indeed, in every port that suffered from lateral spreading there was liquefaction, but the opposite is not necessarily true. An example of lateral spreading is presented for the North Coronel pier in Figure 2.3, which was severely damaged in the approach zone. This zone is composed of a 30 cm thick RC deck supported on $\phi=46$ cm (18 in) (vertical) and $\phi=56$ cm (22 in) (battered) 9.5 mm thick steel piles. The forces induced by the displacement of the soil mass at the shore exceeded the support capacity and pushed the first four lines of piles by approximately 14 degrees. Ten millimeter steel plates welded to the web and flanges of the transverse beams, buckled and yielded. Welding at the pile caps of many piles fractured in shear, causing pile displacements of up to 3 m, and leaving a 22 m beam span unsupported.

Damage in battered piles was also common in most of the observed piers. Since battered piles are intended for resisting lateral earthquake loads and mooring, berthing and crane operations, they are significantly stiffer laterally than vertical piles and, hence, attract larger earthquake forces. Therefore, ductility and displacement capacity are a main concern in the design of these RC piles (PIANC, 2001). Two other concepts are important in interpreting the pier damage in this earthquake: (i) the short pile effect; and (ii) natural torsion. Shorter piles are also stiffer and tend to attract considerably more lateral load than longer piles. As a result, stresses in the top pile-deck joints on the approach zone are generally large (Mondal & Rai, 2008). Because of this larger stiffness provided by the shorter piles, decks tend to rotate relative to the approach zone, increasing the ductility demands of the piles at the seaside edge (Figure 2.4). Battered piles in the transverse direction of the last 96 m of the Huachipato

pier were cut at the connection with the deck; however, no longitudinal battered or vertical piles had structural damage. One plausible explanation would be natural torsion as indicated above, in conjunction with a poor pile-deck connection design and/or implementation. In summary, the approach zone experiences larger force demands, while the berthing zone experiences larger displacement demands.

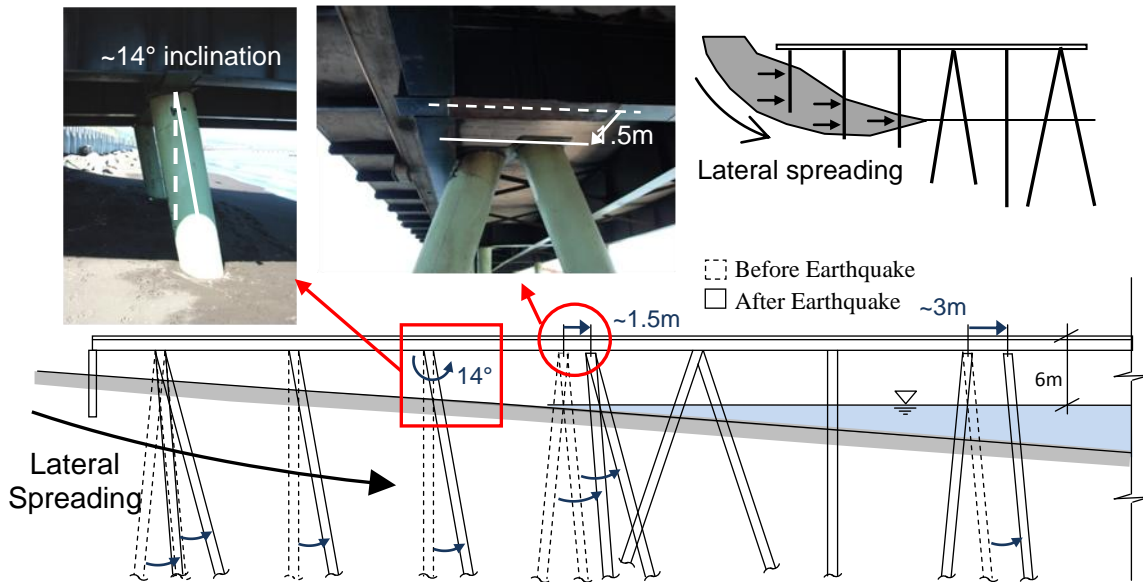


Figure 2.3. Inclination and shear damage of piles located in the approach zone in the North Coronel Pier

Other less frequent structural damage was also present in ports. At the port access or bridge, open-type structures like Jureles, Huachipato, and ENAP piers, showed similar damage. Differential displacements (horizontal or vertical), tilting, and pounding between pier deck and retaining walls, was the cause of fracture, fall and/or collapse of the bridge or other elements located in the access zone. In close-type ports like ASMAR and Talcahuano, quay walls and soil retaining structures underwent large damage. Due to excessive bending moments, the sheet pile wall fractured. Significant horizontal and even vertical cracks developed due to the combined failure of the joint padlocks between the sheet piles. A high corrosion level may have also contributed to this failure. This fact, added to the water effect (tsunami), caused the opening of the cracks and a massive loss and flow of fill material into the sea, resulting in fracture/settlement of the deck and an overall seaward displacement of the anchor system, inducing a large misalignment of the berthing line.

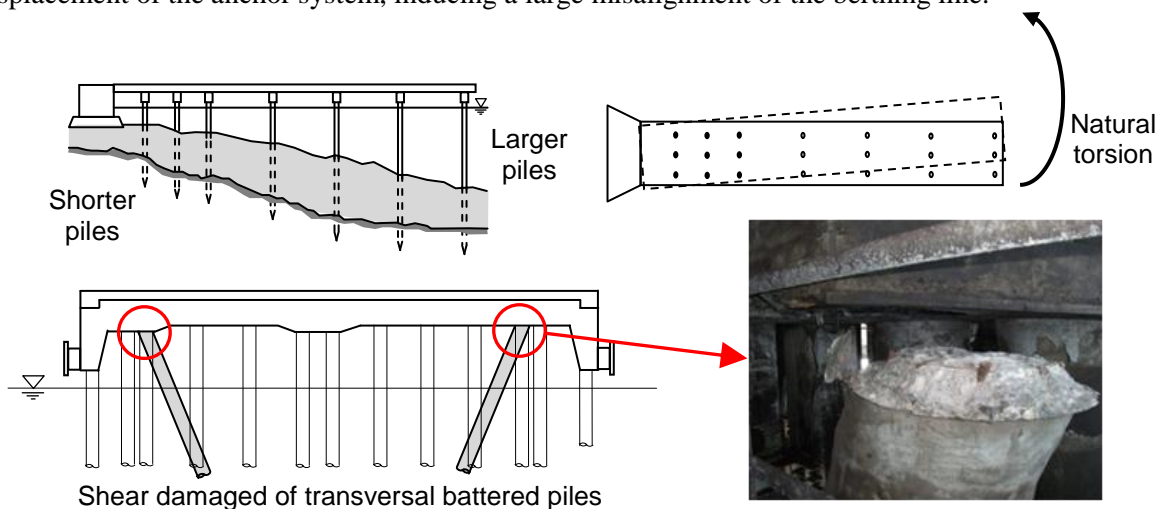


Figure 2.4. Shear damage in transversal battered piles due natural torsion at Huachipato Pier.

The most common non-structural related problems occurred on crane and mooring systems. Two out of three cranes used of the Huachipato Port were damaged; the supporting structures of the cranes are stiff frames which cannot easily withstand relative displacements in the supporting span. Hence, due to the rocking of the cranes, the landside legs of one crane were subjected to excessive compressive forces and bending moments, leading to the formation of a plastic hinge and mechanism, which caused the derailment of the wheels and rupture of the clamps and anchors holding the wheels to the rail. Mooring systems failed because of the strong pull of ships caused by the preventive exit maneuver for the tsunami effect immediately after the earthquake.

3. SEISMIC BEHAVIOR OF SOUTH CORONEL PIER

This section includes a brief description of the earthquake performance of the South Pier of the Coronel port, close to other ports that suffered significant damage. The incorporation of seismic isolation solution in this pier served a double purpose—first, to achieve a cost-effective structural design that reduced the usual number of battered piles to about half, and second, to improve the earthquake performance of the structure and guarantee operational continuity. In fact, the seismic demands on the structure were nominally reduced by a factor between 4 and 5. This design goal was achieved by using a hybrid isolation solution that combines natural rubber isolators placed on top of pyramidal platforms formed by four battered piles (Figure 3.1) and vertical piles working in parallel with the seismic isolators.

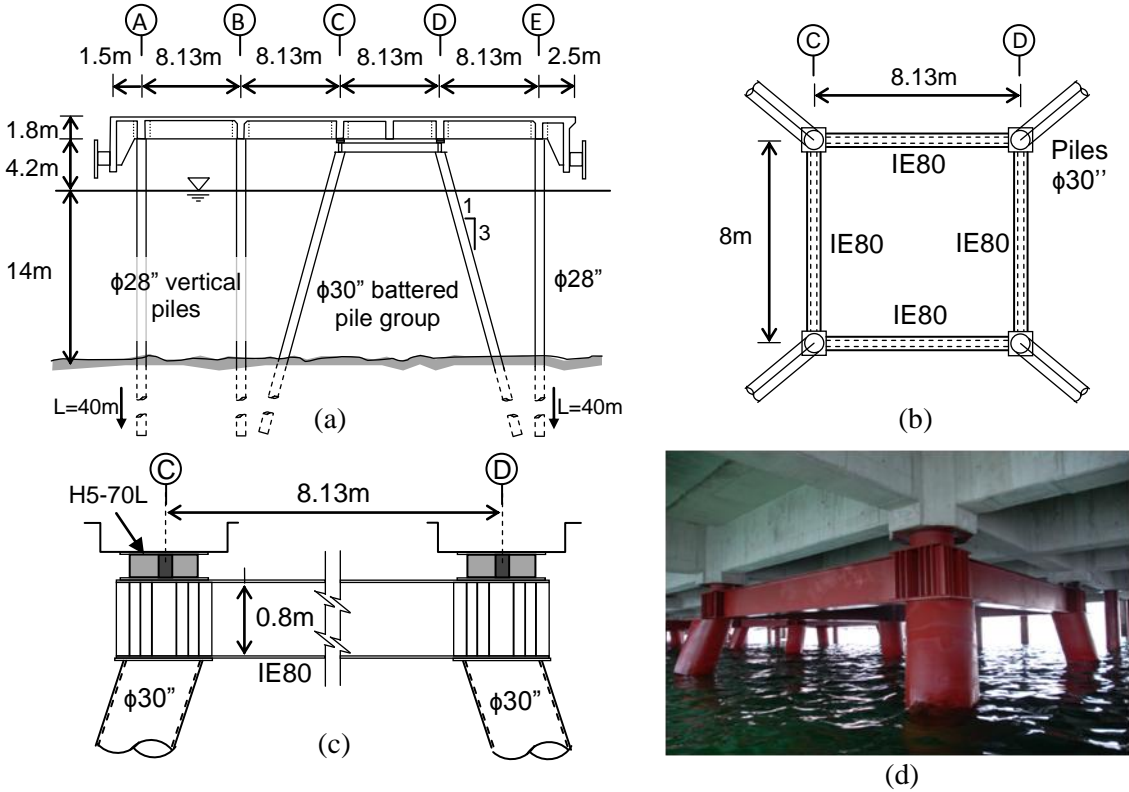


Figure 3.1. (a) Typical cross section of south pier, Coronel; (b) plan view of four battered-pile group; (c) LRB location on four battered pile group; (d) typical four battered pile group.

This pier has a 225.5 m long and 10 m wide reinforced concrete (RC) approach zone, connected to an RC berthing zone 400 m long and 36.5 m wide (Figure 3.2). The lateral resisting system of the berthing platform is formed by 24 pyramidal groups of 4 converging battered piles, and 4 lead-core natural rubber bearings (LRB) on each pile group. Battered piles are connected by steel beams to ensure a stiff substructure that minimizes lateral deformation and thus improving isolator efficiency. A typical transverse elevation of the pier has 3 vertical piles of diameter $\phi=71$ cm (28 in) and 16 mm

thickness, and 2 battered piles of diameter $\phi=76$ cm (30 in) and 20 mm thickness. Vertical piles include a concrete fill in the first 6.5 m under the deck to achieve a good connection between pile and deck.

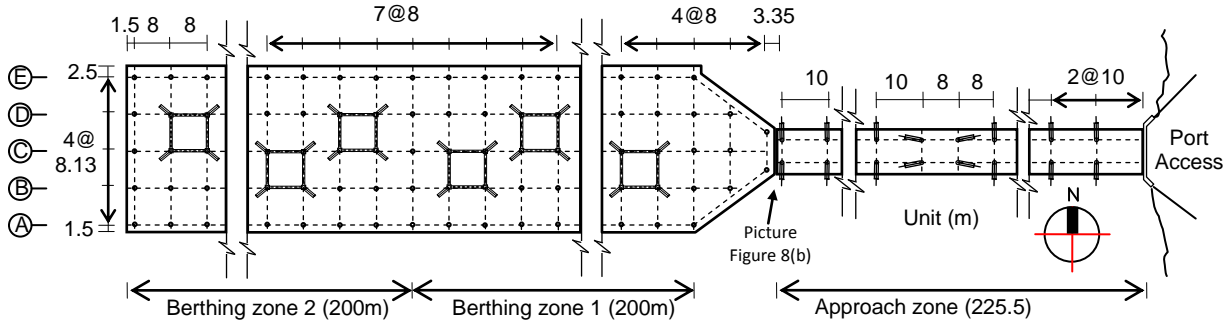


Figure 3.2. Plan view of south pier, Coronel.

A critical aspect in design was the lateral stiffness of the vertical piles, which depended strongly on the soil properties. The soils study included 8 marine boreholes and 1 land borehole, in-situ pile tests, and other laboratory tests on soil properties. One tension and one compression static load test were performed at two different depths along the same pile located inland on the approach zone, and one more compression load test was performed on a pile located on the berthing zone (sea). Additionally, pile driving analyses (PDA) were performed in 16 piles. The longitudinal soil profile was inferred from all tests and measurements, and is represented by four principal soil layers. The soil stratigraphy consisted of a 5 m thick (in average) layer of mud; a second layer of silty sands of medium-to-high density with intermittent lenses of silts and a thickness ranging between 26 m and 30 m; a third layer of slightly plastic silts and high plasticity clays; and a fourth layer of dense fine grain sandstone, with variable cementation from low to very high. Thin layers (less than 3.2 m) of gravel and stones within a sandy matrix were found in a few boreholes just above the bedrock.

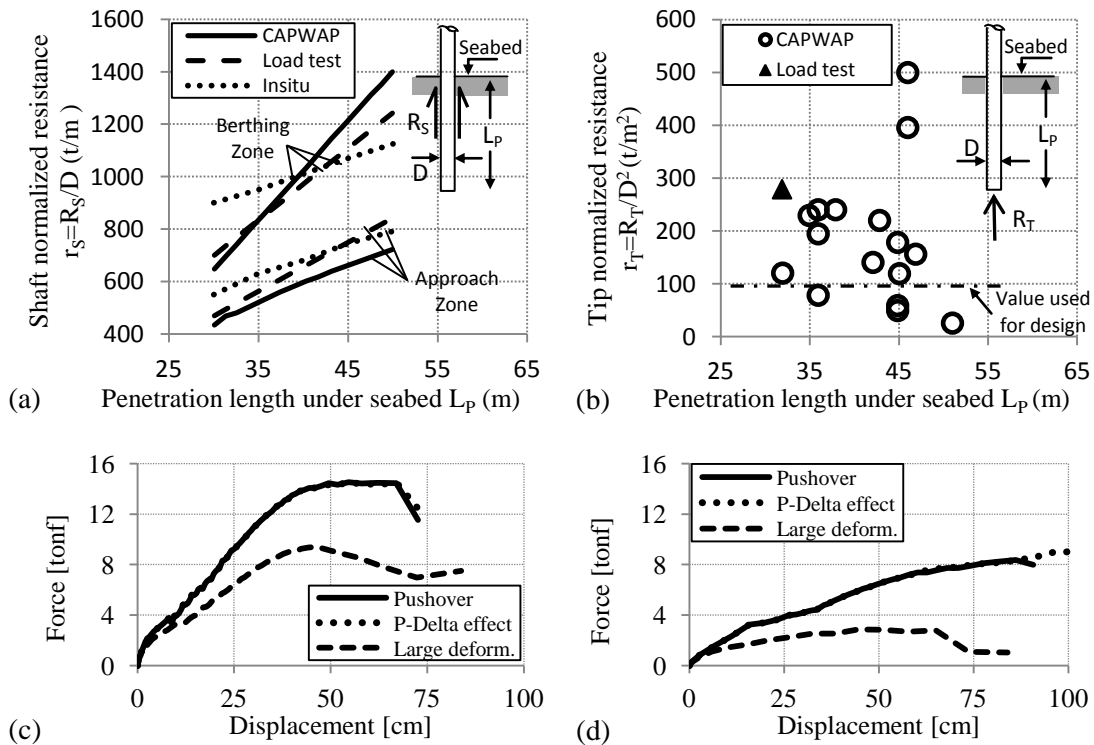


Figure 3.3. Estimated pile behavior: (a) shaft normalized resistance; (b) tip normalized resistance; (c) pushover analysis of a $\phi 28$ vertical pile in infinitely rigid soil; and (d) pushover analysis of a $\phi 28$ vertical pile in infinitely flexible soil.

Shown in Figure 3.3 is the variation of the pile shaft resistance R_S (normalized by the pile diameter D) versus pile penetration length below soil surface. The results obtained from loads tests, in-situ piles tests, and PDA analyses are summarized for the approach zone, and berthing zone. The tip resistance of the pile R_T (normalized by the square of the pile diameter D^2) was obtained at the buried length of the pile within the clay layer.

As stated above, in this hybrid system vertical piles function as “isolator piles” in parallel with the LRB. Design requirements for the vertical piles were: (i) to provide, in conjunction with the isolation system, a combined lateral stiffness consistent with the objective isolated period ($T=3.15$ s); (ii) to be completely stable up to a lateral displacement consistent with that of the isolation system, $D_D=24.3$ cm. This displacement is much larger than the one imposed in a conventional pier with battered piles. Pushover analyses were used to verify the deformation capacity of the pile and the lateral stiffness and stability. Such analyses included the inelastic effect of the soil and large deformations. Two extreme assumptions for the lateral stiffness of the surrounding soil were considered: infinitely rigidity and large flexibility. The pushover was performed on a vertical pile belonging to a typical transverse elevation with 65×160 cm concrete beams and 200 tonf axial load. Results obtained from this model are shown in Figure 3.3. The largest force demand was obtained for infinitely rigid soil; in this model the pile reached a lateral displacement of 40 cm within the elastic range. This displacement enabled the vertical piles to remain elastic for the design isolator displacement D_D .

The 96 seismic isolators were all circular with diameter $\phi=700$ mm, 27 layers of natural rubber of thickness $t_r=6$ mm; the total rubber height was $H_R = 162$ mm. Each rubber layer was separated by steel shims of $t_s=3$ mm thick, and considered a total of 26 steel shims. The lead core was $d_l=100$ mm in diameter, and the lead yield stress $\sigma_l=9.8$ MPa (~ 100 kgf/cm²). The top and base connection plates were square with side $d_p=900$ mm, and $t_p=22$ mm thick end plates. Seismic isolators were connected to the deck and piles through 8 high-strength bolts of diameter $\phi_b=32$ mm (1.25 in).

All seismic isolators were subjected to shear-compression tests to the design displacement $D_D=24.3$ cm, and 2 prototypes to a maximum displacement $D_M=29$ cm. Dynamic testing consisted in the application of 5 full cycles to lateral displacements equivalent to shear deformations $\gamma=\delta/H_R$: (i) $\gamma = 0.25$, (ii) $\gamma = 0.50$, (iii) $\gamma = 1.00$, and (iv) $\gamma = 1.5$. An axial load of 4.12 MN (420 tonf) was applied at all lateral displacements. This load corresponds to the average load for all isolators and the load combination: 1.2D+L+E. Shear forces, lateral stiffnesses, damping ratios, and shear moduli were obtained for all LRBs before and after the introduction of the lead core. A typical force-displacement hysteresis loop obtained for a LRB with and without the lead core is shown in Figure 3.4. Based on these parameters, the resulting isolated period of the pier for a design displacement D_D was $T_D=3.16$ s. Please note from the figure and table that the measured stiffnesses obtained for a typical LRB are slightly higher than the nominal stiffnesses of the vertical piles, and hence, isolators will be subjected to a higher shear force demand than vertical piles.

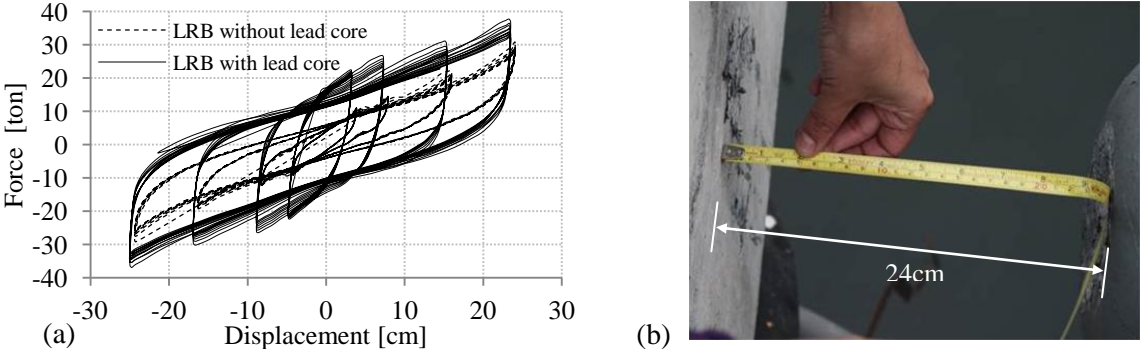


Figure 3.4. (a) Experimental force-displacement hysteresis loop; and (b) relative displacement measured between isolated berthing zone and non-isolated approach zone in South Coronel Pier

During the design process, the inelastic validation of the structure was performed for one of the two isolated segments of the berthing zone using a response history analysis and three different synthetic records generated from seed records of San Felipe, Melipilla and Llo-lleo (Chile, 1985) and compatible with the NCh2745 design spectra (INN, 2003), maximum seismicity zone 3, and soil type II (stiff soil). Shown in Table 2 are the global responses of 200m long and 36.5m wide structure, with a total seismic weight of 186 MN and isolated weight of 172 MN, for the application of the three records in the longitudinal X-direction and transversal Y-direction of the pier, respectively. The apparent periods of the structure at a displacement of 24.9 cm and 24.2 cm for X and Y-directions were identical and equal to $T=3.4$ s, for the San Felipe seed record. The maximum displacement of the center of mass (CM) of the deck was 28.7 cm in both X- and Y-directions, again for the San Felipe seed record. The total seismic shear force for all LRB groups of this section of the pier ($N=48$ LRB) ranges between 14.1 MN and 15.9 MN, which represents between 7.5%-8.5% of the seismic weight of the pier segment. Moreover, the seismic shear taken by the complete substructure, namely the vertical piles and the LRBs, reached a maximum for the San Felipe record of 20.2 MN, i.e., 10.8% of the seismic weight of the structure. Table 2 also shows the maximum lateral deformation, shear, and axial load demand for the LRBs. The estimated maximum X-direction lateral deformation, shear and axial load are respectively, 24.9 cm, 347kN (35.4 tonf), and 1.66 MN (169.2 tonf).

Table 3.1. Global response of the South Coronel Pier

	Synthetic records						Feb. 27, Earthquake	
	San Felipe		Melipilla		Llo-lleo		San Pedro	
Wharf isolated module	X-dir	Y-dir	X-dir	Y-dir	X-dir	Y-dir	X-dir	Y-dir
Period, T (s)	3.40	3.40	2.62	2.62	3.06	3.06	1.96	1.97
Displacement (cm)	28.68	28.62	27.22	27.15	23.65	23.58	17.02	12.54
Isolators shear (tonf)	1624	1623	1571	1570	1440	1439	1196	1032
Isolator+vert. piles shear (tonf)	2065	2055	2000	1989	1803	1793	1475	1223
Most demanded LRB	X-dir	Y-dir	X-dir	Y-dir	X-dir	Y-dir	X-dir	Y-dir
Deformation (cm)	24.92	24.24	23.65	23.01	20.56	19.96	14.83	10.72
Shear (tonf)	35.4	34.8	34.2	33.6	31.3	30.7	25.9	22.0
Axial (tonf)	169.2	150.3	160.5	143.1	139.1	123.9	100.2	66.1

These results should be ideally compared with the ones derived from recorded ground motions in the past February 27, 2010, Maule event. Assuming that the available San Pedro record (Chile, 2010) is representative of the motions in the region (soft soil), the response history results for this record are presented in Table 3.1 just as a reference. The predicted lateral displacements of the CM of the pier for the San Pedro record were 17 cm in the longitudinal and 12.5 cm in the transversal direction. This displacement is less than the one predicted by the NCh2745 design spectrum, but it is consistent with the one observed at the isolation joint shown in Figure 3.4(b). This picture shows that there was pounding at the isolation joint between the isolated berthing zone and a drain pipe mounted on the non-isolated approach zone indicating that the relative displacement between the two structures was at least 24 cm in the longitudinal direction, which represents the sum of the displacements for the berthing and approach zones—the location where the picture was taken is shown in Figure 3.2. The maximum LRB displacement predicted by the model was 14.8 cm, which represents 61% of the design displacement D_D ; a shear force close to 255 kN (26 tonf) (70% of the design value), and apparent response periods of $T=1.96$ s and 1.97s for X- and Y-directions, respectively.

4. LESSONS LEARNED

In general, quantitative procedures to evaluate potential for lateral spreading are not specified by codes; lateral spreading appears mostly as a qualitative concept. To account for it, codes include some basic pseudo-static methods of slope instability and others by a loss in shear strength of the soil. However, details on how this can affect the foundation system are not included. Some recent work

provides guidelines for estimating lateral loads on piles imposed by liquefied layers. These should be incorporated soon in codes to improve the approach to account for lateral spreading.

It was found that code provisions make reference to open type structures just in the case of marginal wharfs. No explicit recommendations exist for large pier structures that run perpendicular to the shore. Therefore, problems such as natural torsion, and short pile effects, are not explicitly considered in codes and design guidelines.

Another interesting design implication is that lateral spreading also induces damage due to beam-deck compression. As the soil next to the approach zone slides, it creates an excessive lateral load on pile foundations. Longitudinal battered piles on the berthing zone located seaward, which has a lower ground slope and no effects of lateral spreading, act like a bracing system restraining the movement of the pier toward the sea. As a result, the longitudinal beams and deck are subjected to a strong compression not considered in the design of the structure.

The right balance of stiffness between vertical piles and isolators on top of battered piles provides an interesting solution to distribute lateral forces among elements. This concept should be included as a design alternative for open-type port structures since it is economic and has proven success in the South Coronel Pier.

Finally, this hybrid isolation solution could also be interesting for ports with piles of different lengths as it occurs naturally for piers that run from the shore and into the sea. In that case, isolation should be on the approach zone and would help homogenize the variability of the longitudinal stiffness along the pier.

5. CONCLUSIONS

Total direct cost in port damage in the Concepción and Talcahuano region was 285 million dollars and could be attributed mainly to a wide variety of soil problems, such as, soil liquefaction and lateral spreading.

A comparison between the analytical results for the design and the observed behavior of the seismically isolated South Coronel Pier shows that the structure was likely subjected to deformations and forces close to 2/3 of their design values. Vertical piles and superstructure stayed within the elastic range, while isolators experienced important nonlinear deformations. Operational continuity of the pier was achieved.

Several design implications of the earthquake observation have been pointed out and hopefully may guide some future research to improve port standards. The dynamic soil structure interaction problem that occur in port structures are very complex in nature and require detailed analyses and substantial further research. This paper has only intended to be mostly of archival nature and a preliminary reference to engineers and researchers involved in this challenging earthquake problem.

ACKNOWLEDGEMENT

This research has been funded by the Chilean Fondo Nacional de Ciencia y Tecnología, Fondecyt, through Grant #1110377. The authors are grateful for this support. The authors are also grateful of the support of the company PRDW Aldunate-Vásquez, responsible for the design of the South Coronel Pier, and Dr. Charles Wicks from the USGS for helping us with the interferometric analysis of the region.

REFERENCES

Barrientos, S. (2010). Terremoto Cauquenes 27 de Febrero 2010. Informe técnico actualizado 27 de Mayo 2010, Universidad de Chile, 20p. URL: www.sismologia.cl

- INN Instituto Nacional de Normalización. (1996). *NCh433 Of.96 Diseño Sísmico de Edificios*. Chile.
- INN Instituto Nacional de Normalización. (2003). *NCh2745 Of.2003 Análisis y Diseño de Edificios con Aislación Sísmica*. Chile.
- MOP Ministerio de Obras Públicas. (2005). Sistema Portuario de Chile 2005. *Government Report*,
[URL:www.mop.cl](http://www.mop.cl)
- Mondal, G., & Rai, D. C. (2008). Performance of harbour structures in andaman islands during 2004 sumatra earthquake. *Engineering Structures*, 30(1), 174-182. DOI: 10.1016/j.engstruct.2007.03.015
- PIANC. (2001). *Seismic design guidelines for port structures*.
- Ruegg, J. C., Rudloff, A., Vigny, C., Madariaga, R., de Chabaliér, J. B., Campos, J., Kausel, E., Barrientos, S., Dimitrov, D. (2009). Interseismic strain accumulation measured by GPS in the seismic gap between constitucion and concepcion in chile. *Physics of the Earth and Planetary Interiors*, 175(1-2), 78-85.
- U.S. Geological Survey. (2010). Finite fault model.
[URL:earthquake.usgs.gov/earthquakes/eqinthenews/2010/us2010tfan/finite_fault.php](http://earthquake.usgs.gov/earthquakes/eqinthenews/2010/us2010tfan/finite_fault.php)
- U.S. Geological Survey. (2010). *M8.8 offshore bio-bio, chile, earthquake of 27 february 2010*.